Title

Biomechanics of osteochondral impact with cushioning and graft Insertion: Cartilage damage is correlated with delivered energy

Authors

Su, Alvin W
Chen, Yunchan
Dong, Yao
et al.

Publication Date

2018-05-01

DOI

10.1016/j.jbiomech.2018.03.037

Peer reviewed

HHS Public Access

Author manuscript

J Biomech. Author manuscript; available in PMC 2019 May 17.

Published in final edited form as:

J Biomech. 2018 May 17; 73: 127–136. doi:10.1016/j.jbiomech.2018.03.037.

Biomechanics of Osteochondral Impact with Cushioning and Graft Insertion: Cartilage Damage is Correlated with Delivered Energy

Alvin W. Su, M.D., Ph.D.[a], **Yunchan Chen**[b], **Yao Dong**[b], **Dustin H. Wailes, B.S.**[b], **Van W. Wong, B.S.**[b], **Albert C. Chen, Ph.D.**[b], **Shengqiang Cai, Ph.D.**[a,c], **William D. Bugbee, M.D.**[e,f], and **Robert L. Sah, M.D., Sc.D.**[a,b,d,e]

[a]Materials Science and Engineering Graduate Program, University of California, San Diego, La Jolla, CA, USA

[b]Department of Bioengineering, University of California, San Diego, La Jolla, CA, USA

[c]Department of Mechanical and Aerospace Engineering, University of California, San Diego, La Jolla, CA, USA

[d]Department of Orthopaedic Surgery, University of California, San Diego, La Jolla, CA, USA

[e]Center for Musculoskeletal Research, Institute of Engineering in Medicine, University of California, San Diego, La Jolla, CA, USA

[f]Department of Orthopaedic Surgery, Scripps Clinic, La Jolla, CA, USA

Abstract

Articular cartilage is susceptible to impact injury. Impact may occur during events ranging from trauma to surgical insertion of an OsteoChondral Graft (OCG) into an OsteoChondral Recipient site (OCR). To evaluate energy density as a mediator of cartilage damage, a specialized drop tower apparatus was used to impact adult bovine samples while measuring contact force, cartilage surface displacement, and OCG advancement. When a single impact was applied to an isolated (non-inserted) OCG, force and surface displacement each rose monotonically and then declined. In each of five sequential impacts of increasing magnitude, applied to insert an OCG into an OCR, force rose rapidly to an initial peak, with minimal OCG advancement, and then to a second prolonged peak, with distinctive oscillations. Energy delivered to cartilage was confirmed to be higher with larger drop height and mass, and found to be lower with an interposed cushion or OCG insertion into an OCR. For both single and multiple impacts, the total energy density delivered to the articular cartilage correlated to damage, quantified as total crack length. The corresponding fracture toughness of the articular cartilage was 12.0mJ/mm^2. Thus, the

Corresponding Author Robert L. Sah, M.D., Sc. D., University of California-San Diego, Department of Bioengineering, 9500 Gilman Drive, Mail Code 0412, La Jolla, CA 92093-0412, Ph: 858-534-0821, Fax: 858-822-1614, rsah@ucsd.edu.

Conflict of interest statement

All authors declared no conflict of interest.

biomechanics of OCG insertion exhibits distinctive features compared to OCG impact without insertion, with energy delivery to the articular cartilage being a factor highly correlated with damage.

Keywords

Articular Cartilage; Cartilage Mechanics; Impact Mechanics; Osteochondral Autograft; Osteochondral Allograft

1. Introduction

Articular cartilage is susceptible to impact injury, such as that occurring in traumatic events or surgical procedures like osteochondral graft (OCG) insertion. Such injury may lead to post-traumatic osteoarthritis (Anderson et al., 2011). Understanding the mechanobiological factors that cause such damage to the cartilage may aid in prevention or treatment. Two key features of cartilage damage due to impact are fissure formation (Ewers et al., 2001; Jeffrey et al., 1995; Repo and Finlay, 1977) and chondrocyte death (Loening et al., 2000; Repo and Finlay, 1977; Szczodry et al., 2009; Torzilli et al., 1999).

Various mechanical factors during impact have been suggested as causative of cartilage damage. Cartilage matrix damage and chondrocyte death have been associated with impact force (Kang et al., 2010; Patil et al., 2008; Whiteside et al., 2005), contact stress (Repo and Finlay, 1977; Torzilli et al., 1999), compressive stress rate (Ewers et al., 2001; Milentijevic and Torzilli, 2005), compressive strain (Repo and Finlay, 1977; Torzilli et al., 2006), compressive strain rate (Quinn et al., 2001), and total impact energy (Burgin and Aspden, 2008 ; Finlay and Repo, 1979 ; Szczodry et al., 2009). Studies of OCG insertion into OCR from human cadavers *ex vivo* (Borazjani et al., 2006; Patil et al., 2008), in animals *in vivo* (Pallante et al., 2012), and in models *in vitro* (Pylawka et al., 2007; Whiteside et al., 2005) have focused on applied energy, force, impulse, and the number of taps required for insertion. However, the biomechanics of energy transmission and dissipation during OCG impact insertion, and its relation to articular cartilage damage, are unclear.

With cartilage impact and OCG insertion, articular cartilage damage may be associated with the energy density transmitted to the cartilage. Energy density has been analyzed as energy normalized either to articular cartilage surface contact area (Heiner et al., 2013; Martin et al., 2009) or to cartilage volume (Burgin and Aspden, 2008 ; Finlay and Repo, 1979). However, during OCG insertion into an OCR, energy can be absorbed by structures other than the articular cartilage, particularly the interacting bone between the OCG and OCR.

To elucidate OCG insertion biomechanics and the possible role of delivered energy in causing cartilage damage, two experiments were performed with a specially instrumented drop-tower apparatus. (1) Isolated OCGs were impacted at two energy levels, with or without an interposed cushion to provide a series compliance, somewhat like an OCR, to modulate the delivered energy. (2) OCGs were inserted into OCRs by five sequential impacts of increasing energy. Impact of isolated OCGs tests an approach to assess energy delivered to cartilage, modulated by cushion or drop height, while approximating the situation where

an impact is insufficient to cause OCG advancement. Impact insertion of OCGs into OCRs tests mechanical mechanisms of energy storage or dissipation, diverting energy from the cartilage. Both test if lessened cartilage strain energy reduces cartilage damage.

2. Methods

2.1. Study Design

In two experiments, the effects of OCG impact (Fig. 1) on a number of biomechanical variables (Table 1) were quantified, based on measurement of axial load, $F(t)$, and cartilage surface displacement, $u^{AC}(t)$, along with optical visualization of the samples in between the impact and insertion events. Subsequently, biological damage to articular cartilage was assessed, primarily, as total crack length, L_{crack}.

Experiment 1—During OCG impact, the effects of total applied (potential) energy density, W_S^{PE}, and cushioning on biomechanical variables as well as damage to the OCG articular cartilage were analyzed for four groups, each with n=6 samples, (1) W_S^{PE}=7.6mJ/mm^2, without cushioning, (2) W_S^{PE}=7.6mJ/mm^2 with cushioning, (3) W_S^{PE}=22.9mJ/mm^2, without cushioning, and (4) W_S^{PE}=22.9mJ/mm^2, with cushioning. The two levels of W_S^{PE} were chosen, based on pilot studies, to cause mild and severe cartilage damage, respectively. The cushioning was provided by a 3.2mm thick, 12mm diameter disc of 40-Durometer silicone-rubber, placed atop the loading tamp. The cushion was chosen so that its structural stiffness, 190N/mm, was similar to the stiffness of the OCG under the tested impact conditions, with the expectation of diverting approximately half of the applied energy from the OCG to the cushion. Damage was assessed, secondarily, as articular cartilage area, $A^{AC}(t_{24hr+})$.

Experiment 2—During sequential OCG impact, the effects of insertion on biomechanical variables as well as damage to articular cartilage were analyzed with two study groups, each with n=3 samples, (1) non-insertion impact of an isolated OCG (similar to *Experiment 1*), and (2) insertion of an OCG into an OCR, as well as for a non-loaded control group for viability analysis (n=6). Five levels of W_S^{PE}, 0.9, 1.3, 2.0, 3.0, and 4.5mJ/mm^2 (increasing by a factor of ~1.5) were applied sequentially to the OCG, based on preliminary studies (and confirmed in the present study) indicating that such an impact sequence was sufficient to advance the OCG into the OCR incrementally, while leaving the OCG slightly proud after the 5th (last) tap. Damage was assessed, secondarily, as viability of chondrocytes at the cartilage surface, V^{AC}.

2.2. Detailed Experimental Methods

OCG and OCR Preparation—A total of 36 OCGs and 3 OCRs were prepared from a total of six adult bovine knees, essentially as described previously (Chen et al., 2001). The OCGs had a subchondral bone radius, a^{SCB}, of 2.40mm and a subchondral bone thickness, h^{SCB}, of 5.0mm. The radius of the articular cartilage of the 24 OCGs for *Experiment 1* was 1.50mm, and that of the 12 OCGs for *Experiment 2* was 2.40mm. The OCR bone sockets had radius, a^{OCR}, of 2.40mm and depth from the articular surface, h^{OCR}, of 10mm. (See Supplement.)

Impact Loading and OCG Insertion—A drop tower, combining features of previous designs to assess impact mechanics (Burgin and Aspden, 2007; Finlay and Repo, 1978; Jeffrey et al., 1995), was used to apply impact load with known potential energy to the OCGs and obtain measures of biomechanical variables (Fig. 1A). Impact was delivered by dropping a mass, m, from height, h^{drop}, onto a tamp, placed on the articular surface of an OCG, with an in-line piezoelectric load cell (PCB208C05, PCB-Piezotronics, Depew, NY) and a laser displacement sensor (Acuity-AR200, Schmitt Industries, Portland, OR) to monitor cartilage surface loading and position, respectively. The tamp (0.050kg) was made out of stainless steel with flat surfaces (diameter=12mm) at both ends. (See Supplement.)

Cartilage Thickness and Area Measurements—OCG cartilage thickness, before and after impact, $h^{AC}(t_{0-})$ and $h^{AC}(t_{24hr+})$, respectively, were determined by imaging the samples, as were cartilage surface areas, $A^{AC}(t_{0-})$ and $A^{AC}(t_{24hr+})$. (See Supplement.)

Mechanical Data Acquisition and Analysis—Mechanical quantities were computed from the parameter values and measured variables (Figs. 1,2). The drop mass, m, was 0.545kg, and the drop heights, h^{drop}, ranged from 3.5–51.8 mm. Total applied energy, W^{PE}, was computed as potential energy, $m{\cdot}h^{drop}{\cdot}g$, with an accuracy and precision of 2–17% at high-low drop heights (e.g., 0.5mm resolution / 30–3 mm drop height). The contribution of energy associated with the lowering of the tamp was considered negligible, as it was <2% of W^{PE} based on mass and movement; however, the drop energy, $W^{PE,Tot}$, in *Experiment 2* included that due to the non-negligible OCG advancement into the OCR site. W^{PE} and $W^{PE,Tot}$ were normalized to contact surface area, $A^{AC}(t_{0-})$, to yield the applied (area-averaged) energy density, W_S^{PE} and $W_S^{PE,Tot}$.

The various mechanical indices were determined for each impact, relative to tare or initial values. The time point of impact, $t=0$, was taken as when $F(t)$ became greater than 0.5N, a small value relative to impact-related forces (e.g., Figs. 2A,2D). The force, $F(t)$, and tamp position, $u^{Tamp}(t)$, were determined relative to tare values (averaged over the 2 ms prior to impact). When contact force reached it's peak, the time, t_{Fp}, and force, F_p, were recorded. Peak contact stress, σ_p, was calculated as F_p normalized to $A^{AC}(t_{0-})$. The duration of loading, T, was determined as the time interval between the times before and after t_{Fp} at which $F(t)$ was half of F_p. The impulse, I, of the impact event was calculated by integrating $F(t)$ over that time period, T (Fig. 2A).

The tamp position, $u^{Tamp}(t)$, was monitored to assess the axial displacement of the articular cartilage surface of OCGs. The axial displacement of the OCG subchondral bone was considered negligible, based on the compressive modulus being ~1000× higher for bone (Rho et al., 1993) than articular cartilage (Korhonen et al., 2002; Schinagl et al., 1997), and thickness being only ~4–10× greater for the bone than the cartilage of the OCG and OCR samples. Thus, during impact of the isolated OCG in *Experiments 1* and *2*, $u^{Tamp}(t)$ was taken as equivalent to axial displacement of the cartilage surface, $u^{AC}(t)$ (Figs. 1A–ii,2B), as were the peak displacement values, u_p^{Tamp} and u_p^{AC}, occurring at time point, t_{up}.

For impact insertion of OCGs into OCRs in *Experiment 2*, for each tap, i, in the series of five taps, the measures for an individual tap are shown exactly as for *Experiment 1*, or with

an appended "*[i]*" when a particular tap or series of taps is described. The incremental graft advancement distance, $u_{adv}[i]$, for each tap, i, was taken as the change in axial position of the OCG articular surface, as determined from photographs (0.02mm pixel resolution) before and after impact i, relative to the OCR articular surface (Fig. 3). Since $F(t)$ was at an approximately constant plateau value (e.g., during t=1–7ms in Fig. 2D) while the tamp was advancing the OCG into the OCR (Fig. 2E), the peak displacement of cartilage surface relative to subchondral bone of such OCGs was estimated as the difference between tamp movement and graft advancement, $u_p^{AC}[i]=u_p^{Tamp}[i]-u_{adv}[i]$ (Figs. 1B–ii,2E). Peak axial strain of the articular cartilage ($\varepsilon_p[i]$) was thus calculated as $u_p^{AC}[i]$ normalized to $h^{AC}(t_{0-})$.

The force-displacement profiles were analyzed to assess mechanical work and energy transfer. The work provided by the tamp during impact, W^{Tamp} (the area under the curve in Figs. 2C,2F), was determined by integrating $F(t)$ over $u^{Tamp}(t)$, from zero until u_p^{Tamp}. The energy dissipated (not returned), W_d (the area of the hysteresis loops in Figs. 2C,2F), was determined by integrating $F(t)$ over $u^{Tamp}(t)$, from zero until the position at which the force returned to zero. For the isolated OCG samples, assuming the bone to be rigid, W^{Tamp} and W_d were taken to be equivalent to the energy delivered to, and dissipated in, the articular cartilage, W^{AC} and W_d^{AC}, respectively. W^{Tamp} was assumed to be divided into W^{AC} and work to advance the OCG into the OCR. Based on the relatively constant $F(t)$ during most of the displacement (Fig. 2F), W^{Tamp} was assumed to be apportioned to the cartilage by the peak deformation of cartilage relative to the movement of bone, with $W^{AC}=W^{Tamp}\bullet(u_p^{AC}/u_p^{Tamp})$. Analogously, W_d was assumed to be apportioned by $W_d^{AC}=W_d\bullet(u_p^{AC}/u_p^{Tamp})$. The delivered and dissipated energies, W^{AC} and W_d^{AC}, were then normalized to $A^{AC}(t_{0-})$ to obtain the energy densities (relative to surface area), delivered to and dissipated by the cartilage, W_S^{AC} *and* $W_{S,d}^{AC}$, respectively (Fig. 2C).

In *Experiment 2*, to enable assessment of the effects of multiple taps on cartilage damage, the above quantities, as well as maximal and cumulative quantities, were assessed. The maximal energy density delivered to OCG samples, $W_{S,max}$, the maximal impact impulse, I_{max}, and the maximal peak contact stress, $\sigma_{p,max}$, were defined as the maximum of the five values from taps 1–5, of W_S, I and σ_p, respectively. For taps i=1–5, cumulative values were computed for energy density delivered to OCG samples, $\sum W_s = \sum_{i=1}^{5} W_s[i]$, impact impulse, $\sum I = \sum_{i=1}^{5} I[i]$, and peak contact stress, $\sum \sigma_p = \sum_{i=1}^{5} \sigma_p[i]$.

Cartilage Crack Formation—L_{crack} was determined as half of the total length of all crack edges visible at the articular surface. Samples were stained with India Ink (Chang et al., 1997), imaged *en face* by reflected light microscopy, and analyzed with NIH ImageJ software for total length of all crack edges (Su et al., 2017). L_{crack} was taken as the average from three independent observers (intra-class correlation coefficient of 0.98).

Chondrocyte Viability—V^{AC}, was determined as (live cells)/(live cells+dead cells) in the central areas of the articular cartilage surface. Cartilage was isolated from bone, incubated for 24 hr in tissue culture medium including 10% FBS, stained with LIVE/DEAD® dye, imaged *en face* in the central 3.75×0.75 mm^2 area using fluorescence microscopy, and

analyzed for live and dead cells by image processing (Borazjani et al., 2006; Pallante et al., 2009; Su et al., 2017).

Statistics—The effects on mechanical variables of W_S^{PE} and cushioning in *Experiment 1* were assessed by two-way ANOVA, and of insertion (at each tap and cumulatively) on mechanical variables and V^{AC} in *Experiment 2* were assessed by t-test and one-way ANOVA, respectively. The dependencies of L_{crack} on mechanical variables were assessed by linear regression. Significance was set at α=0.05. (See Supplement.)

3. Results

Experiment 1

The descriptive and comparative statistics of the measured and computed variables are given in Table 2, and their time-dependent variations are given in Fig. 4. Effects of W_S^{PE} and cushioning on force and stress, displacement and strain, energy, and cartilage damage, are summarized below.

The impact force profile was affected by both W_S^{PE} and cushioning, without interactive effects (Fig. 4A). With higher W_S^{PE}, F_p, and therefore σ_p, were higher, while cushioning had opposite effects. Also, higher W_S^{PE} resulted in a lower t_{Fp} and shorter T, while cushioning had opposite effects (Fig. 4A). However, higher W_S^{PE} and cushioning both resulted in higher I.

The resulting cartilage deformation profile was also affected by W_S^{PE} and cushioning (Fig. 4B). Higher W_S^{PE} resulted in higher u_p^{AC} and ε_p^{AC}, while cushioning resulted in lower u_p^{AC} and ε_p. While t_{up} did not vary independently with W_S^{PE} or cushioning (Fig. 4B, Table 2), there was an interactive effect. Both W^{AC} and W_d^{AC}, and therefore W_S^{AC} and $W_{S,d}^{AC}$, were higher in samples loaded with higher W_S^{PE} and without cushioning (Fig. 4C).

The resultant L_{crack} was higher with higher W_S^{PE} and without cushioning (Fig. 4D–E, Table 2). Without cushioning, the 3-fold higher W_S^{PE} resulted in approximately 3-fold larger L_{crack}. At the low and high W_S^{PE} levels, cushioning led to lower L_{crack}, by 83% and 50%, respectively. Cartilage thickness (all samples) before impact, $h^{AC}(t_{0-})$ was 1.54 mm and did not differ among the four study groups, and increased slightly 24 hours after impact. $A^{AC}(t_{24hr+})$ was larger with higher W_S^{PE} and smaller with cushioning, with an interactive effect.

As summarized in Table 2, W^{AC}, and thus W_S^{AC}, were the mechanical variables most closely correlated with the extent of cartilage damage. L_{crack} was correlated strongly with W_S^{AC}(R^2=0.91, Fig. 5A), σ_p (R^2=0.88, Fig. 5B) as well as $W_{S,d}^{AC}$ (R^2=0.89), and correlated moderately with ε_p^{AC} (R^2=0.53, Fig. 5C) and T (R^2=0.45, Fig. 5D) (each $p<0.001$). L_{crack} was correlated weakly with $W_S/W_S^{PE,Tot}$ (R^2=0.38, $p<0.05$, Fig. 5E) and I (R^2=0.19, $p<0.05$, Fig. 5F).

Experiment 2

Impact mechanics were different between non-insertion and insertion samples, and these differences decreased gradually with tap number (Table 3A). With each tap, $F(t)$ rose rapidly an initial peak at ~1ms with minimal OCG advancement; subsequently, $F(t)$ declined and then rose to a second prolonged peak, with distinctive oscillations during a duration of 5–10 ms. Compared to non-insertion impact, insertion resulted in lower F_p and σ_p, but longer T (Fig. 6A). I was not different except for tap #1, where it was lower with insertion. Insertion resulted in higher u_p^{Tamp}(Fig. 6B), except for tap #5. u_p^{AC} and ε_p were not different except for tap #3, with both being lower with insertion. With each tap, insertion resulted in lower W and therefore W_S (Fig. 6C). W_d^{AC} and $W_{S,d}^{AC}$ were lower with insertion for tap #3 and #4.

Repeated impacts resulted in cartilage matrix damage that was less in OCG that were inserted into OCR than in OCG that were not inserted. L_{crack} was ~30 times higher in non-inserted samples than inserted samples (Fig. 6D). The cumulative quantity, ΣW_S, was three times higher in non-inserted samples than in inserted samples. $h^{AC}(t_{0-})$ was not different between the two groups.

Cell viability was protected by insertion. Relative to non-impacted control samples where viability was 97±3%, V^{AC} was reduced to 88±6% in non-inserted samples ($p<0.05$), with cell death being localized both diffusely and adjacent to cracks (Fig. 6E,F). Insertion had protective effect, with V^{AC} of 95±3% being indistinguishable ($p=0.45$) from control samples, and higher than non-inserted samples ($p<0.05$).

As summarized in Table 3B, L_{crack} was strongly correlated with ΣW_S ($R^2=0.99$, $p<0.001$, Fig. 7D) and $W_{S,max}$ ($R^2=0.93$, $p<0.01$, Fig. 7A), moderately correlated with $\Sigma\sigma_p$ ($R^2=0.75$, $p<0.05$, Fig. 7E), not correlated with $\sigma_{p,max}$ ($p=0.09$, Fig. 7B), I_{max} ($p=0.67$, Fig. 7C), or ΣI ($p=0.55$, Fig. 7F).

Comparison of Cartilage Matrix Damage with Energy Density in Experiments 1 and 2

The correlation of cartilage matrix damage with delivered energy density was similar for OCG in *Experiment 1* and *Experiment 2*. The slopes ($p=0.09$) and the intercepts ($p=0.72$) were not different for L_{crack} versus W_S in *Experiment 1* (Fig. 5A) and for L_{crack} versus ΣW_S in *Experiment 2* (Fig. 7D).

4. Discussion

These results delineated the biomechanical dynamics of OCG impact and its consequences, in the configurations of an isolated (non-inserted) sample and of a sample inserted into an OCR. The amplitudes and time courses of reaction force were modulated by an interposed cushion and by insertion into an OCR, as were the amplitude and time course of cartilage displacement. With additional assessment of graft displacement, the energy delivered to the OCG was estimated. In these impact situations, damage to the articular cartilage, in the form of surface crack formation, was strongly correlated with energy density delivered to the sample (W_S, $\Sigma W_{S,i}$). Damage to OCG cartilage was less with interposition of a cushioning structure that absorbed much of the applied (potential) energy of a dropped mass. Similarly, OCG cartilage damage, including cell death resulting from sequential impact was less when

the OCG was inserted into an OCR, which also absorbed energy, compared to the non-insertion condition. As the OCG advanced deeper into the OCR with increasing tap number and associated increasing resistance to graft advancement, the impact mechanics began to approximate the non-insertion condition.

The study design considered a number of experimental and theoretical issues. Experimentally, as noted in the methods, the accuracy and precision of the applied energy was modest for low drop heights (±2–17%). Also in *Experiment 2*, the estimate of W^{AC} and W_d^{AC} from W^{Tamp} and W_d^{Tamp}, respectively, were based on the peak axial displacements of the cartilage surface and OCG bone during insertion; more exact assessment of these variables would have required simultaneous assessment of articular cartilage compression (not just movement) and OCG displacement, along with *F(t)*. Further, *Experiment 2* was designed so that the OCG would receive impacts sufficient to advance sequentially, but not "bottom out."

The effects of an interposed cushion on impact mechanics of an OCG were somewhat similar to the effects of OCG insertion into an OCR and also distinct from the effects of a lesser drop height. The effects of cushion insertion included a lowering of energy delivery to the sample, prolongation of impact duration, and lowering of peak contact stress. Similar effects were evident with OCG insertion into an OCR, where portions of applied energy are transformed to work that advances the graft or that is dissipated or stored at the host-graft junction due to friction or tissue deformation. In contrast, the impact duration was not affected by a lesser drop height, as noted above. A distinction between the cushion and OCG insertion were the *F(t)* profiles, where insertion was associated with temporal oscillations. Such oscillations may be indicative of transient trabecular interdigitation and deformation, as the OCG advances into and interacts with the OCR. In the cases of both the cushion and OCG insertion, the applied energy that is delivered to the articular cartilage can cause damage. Impact load may be delivered experimentally by alternative devices that store and release energy with spring constructs (Alexander et al., 2013; Bonnevie et al., 2015; Whiteside et al., 2005), which may result in distinct load profiles.

The impact energy delivered to the articular cartilage can be transformed into cracks and their associated free surface energy, when the local energy delivered to the material overcomes the toughness of the material (Anderson, 1995). In the present study, the fracture toughness of cartilage of OCGs averaged 12.0mJ/mm^2, as determined by normalizing $W_{S,d}$ to total crack surface area, assuming that all cracks extended through the full thickness of cartilage. This value is greater than the 0.14–1.50mJ/mm^2 deduced in a canine model using a modified single edge notch test (Chin-Purcell and Lewis, 1996), but lower than 36–58mJ/mm^2 required to shear cartilage off the osteochondral junction in adult bovine explants (Broom et al., 1996). It is also consistent with cartilage matrix damage being noted after impact of isolated cartilage tissue or osteochondral cores, with applied energy densities of 10–50mJ/mm^2 (Heiner et al., 2013; Jeffrey et al., 1995; Szczodry et al., 2009). Differences in cartilage fracture initiation, location, and propagation, and in the animal species tested, may contribute to variations in apparent fracture toughness.

The protection of chondrocytes at the articular surface by cushioning in *Experiment 2* was somewhat consistent with thresholds described in previous studies. The cumulative energy of impacts of *Experiment 2* were above the energy density of 1mJ/mm^3, suggested as the "threshold" for chondrocyte death (Repo and Finlay, 1977). Impact energies were also within the range where a dose-response relationship was noted between applied energy densities of 0.9–102 mJ/mm^2 and the depth of cell death in osteochondral cylinders (Whiteside et al., 2005). Thus, it was not surprising that chondrocyte viability was protected by insertion to reduce the applied energy. The spatial distribution of impact-induced chondrocyte death is complex, with local stress concentrations consistent with causing cell death adjacent to the cracks (Ewers et al., 2001; Repo and Finlay, 1977). At lower energies, even without cartilage failure and crack formation, localized biomechanics critically affects chondrocyte viability (Bae et al. 2007; Bartell et al. 2015). This may explain the lack of correlation between L_{crack} and V^{AC} in the present study.

In summary, the impact insertion of OCG exhibits distinctive biomechanical features compared to OCG impact without insertion. In addition, the energy delivered to the articular cartilage of the OCG, whether inserted or not, correlates strongly to cartilage failure in the form of crack formation. These results imply that the energy of insertion impacts applied to OCG in the standard surgical situation should be kept at sufficiently low levels to prevent cartilage damage. These results imply that the energy of insertion impacts applied to OCG in the standard surgical situation should be kept at levels sufficiently low to prevent cartilage damage. To achieve insertion, more low energy taps could be used instead of relatively few high energy taps. OCG insertion instrumentation system could also be modified to reduce energy delivery to the articular cartilage, such as by applying energy diverting mechanisms, or by reducing of energy dissipation at the OCG-OCR interface while maintaining stability.

Supplementary Material

Refer to Web version on PubMed Central for supplementary material.

Acknowledgments

NIH R01 AR055637 and NIH P01 AG007996.

References

Alexander PG, Song Y, Taboas JM, Chen FH, Melvin GM, Manner PA, Tuan RS. Development of a spring-loaded impact device to deliver injurious mechanical impacts to the articular cartilage surface. Cartilage. 2013; 4:52–62. [PubMed: 26069650]

Anderson DD, Chubinskaya S, Guilak F, Martin JA, Oegema TR, Olson SA, Buckwalter JA. Post-traumatic osteoarthritis: Improved understanding and opportunities for early intervention. J Orthop Res. 2011; 29:802–809. [PubMed: 21520254]

Anderson, TL. Fracture Mechanics: Fundamentals and Applications. 2. CRC Press; Boca Raton, FL: 1995.

Bonnevie ED, Delco ML, Fortier LA, Alexander PG, Tuan RS, Bonassar LJ. Characterization of tissue response to impact loads delivered using a hand-held instrument for studying articular cartilage injury. Cartilage. 2015; 6:226–232. [PubMed: 26425260]

Borazjani BH, Chen AC, Bae WC, Patil S, Sah RL, Firestein GS, Bugbee WD. Effect of impact on chondrocyte viability during the insertion of human osteochondral grafts. J Bone Joint Surg Am. 2006; 88:1934–1943. [PubMed: 16951108]

Broom ND, Oloyede A, Flachsmann R, Hows M. Dynamic fracture characteristics of the osteochondral junction undergoing shear deformation. Med Eng Phys. 1996; 18:396–404. [PubMed: 8818138]

Burgin LV, Aspden RM. A drop tower for controlled impact testing of biological tissues. Med Eng Phys. 2007; 29:525–530. [PubMed: 16876457]

Burgin LV, Aspden RM. Impact testing to determine the mechanical properties of articular cartilage in isolation and on bone. J Mater Sci Mater Med. 2008; 19:703–711. [PubMed: 17619965]

Chang DG, Iverson EP, Schinagl RM, Sonoda M, Amiel D, Coutts RD, Sah RL. Quantitation and localization of cartilage degeneration following the induction of osteoarthritis in the rabbit knee. Osteoarthritis Cartilage. 1997; 5:357–372. [PubMed: 9497942]

Chen AC, Bae WC, Schinagl RM, Sah RL. Depth- and strain-dependent mechanical and electromechanical properties of full-thickness bovine articular cartilage in confined compression. J Biomech. 2001; 34:1–12. [PubMed: 11425068]

Chin-Purcell MV, Lewis JL. Fracture of articular cartilage. J Biomech Eng. 1996; 118:545–556. [PubMed: 8950659]

Ewers BJ, Dvoracek-Driksna D, Orth MW, Haut RC. The extent of matrix damage and chondrocyte death in mechanically traumatized articular cartilage explants depends on rate of loading. J Orthop Res. 2001; 19:779–784. [PubMed: 11562121]

Finlay JB, Repo RU. Instrumentation and procedure for the controlled impact of articular cartilage. IEEE Trans Biomed Eng. 1978; 25:34–39. [PubMed: 621099]

Finlay JB, Repo RU. Energy absorbing ability of articular cartilage during impact. Med Biol Eng Comput. 1979; 17:397–403. [PubMed: 317339]

Heiner AD, Smith AD, Goetz JE, Goreham-Voss CM, Judd KT, McKinley TO, Martin JA. Cartilage-on-cartilage versus metal-on-cartilage impact characteristics and responses. J Orthop Res. 2013; 31:887–893. [PubMed: 23335281]

Jeffrey JE, Gregory DW, Aspden RM. Matrix damage and chondrocyte viability following a single impact load on articular cartilage. Arch Biochem Biophys. 1995; 322:87–96. [PubMed: 7574698]

Kang RW, Friel NA, Williams JM, Cole BJ, Wimmer MA. Effect of impaction sequence on osteochondral graft damage: the role of repeated and varying loads. Am J Sports Med. 2010; 38:105–113. [PubMed: 19915099]

Korhonen RK, Laasanen MS, Toyras J, Rieppo J, Hirvonen J, Helminen HJ, Jurvelin JS. Comparison of the equilibrium response of articular cartilage in unconfined compression, confined compression and indentation. J Biomech. 2002; 35:903–909. [PubMed: 12052392]

Loening A, Levenston M, James I, Nuttal M, Hung H, Gowen M, Grodzinsky A, Lark M. Injurious mechanical compression of bovine articular cartilage induces chondrocyte apoptosis. Arch Biochem Biophys. 2000; 381:205–212. [PubMed: 11032407]

Martin JA, McCabe D, Walter M, Buckwalter JA, McKinley TO. N-acetylcysteine inhibits post-impact chondrocyte death in osteochondral explants. J Bone Joint Surg Am. 2009; 91:1890–1897. [PubMed: 19651946]

Milentijevic D, Torzilli PA. Influence of stress rate on water loss, matrix deformation and chondrocyte viability in impacted articular cartilage. J Biomech. 2005; 38:493–502. [PubMed: 15652547]

Pallante AL, Bae WC, Chen AC, Gortz S, Bugbee WD, Sah RL. Chondrocyte viability is higher after prolonged storage at 37 degrees C than at 4 degrees C for osteochondral grafts. Am J Sports Med. 2009; 37(Suppl 1):24S–32S. [PubMed: 19861697]

Pallante AL, Chen AC, Ball ST, Amiel D, Masuda K, Sah RL, Bugbee WD. The in vivo performance of osteochondral allografts in the goat is diminished with extended storage and decreased cartilage cellularity. Am J Sports Med. 2012; 40:1814–1823. [PubMed: 22707746]

Patil S, Butcher W, D'Lima DD, Steklov N, Bugbee WD, Hoenecke HR. Effect of osteochondral graft insertion forces on chondrocyte viability. Am J Sports Med. 2008; 36:1726–1732. [PubMed: 18490471]

Pylawka TK, Wimmer M, Cole BJ, Virdi AS, Williams JM. Impaction affects cell viability in osteochondral tissues during transplantation. J Knee Surg. 2007; 20:105–110. [PubMed: 17486901]

Quinn TM, Allen RG, Schalet BJ, Perumbuli P, Hunziker EB. Matrix and cell injury due to sub-impact loading of adult bovine articular cartilage explants: effects of strain rate and peak stress. J Orthop Res. 2001; 19:242–249. [PubMed: 11347697]

Repo RU, Finlay JB. Survival of articular cartilage after controlled impact. J Bone Joint Surg Am. 1977; 59-A:1068–1076.

Rho JY, Ashman RB, Turner CH. Young's modulus of trabecular and cortical bone material: ultrasonic and microtensile measurements. J Biomech. 1993; 26:111–119. [PubMed: 8429054]

Schinagl RM, Gurskis D, Chen AC, Sah RL. Depth-dependent confined compression modulus of full-thickness bovine articular cartilage. J Orthop Res. 1997; 15:499–506. [PubMed: 9379258]

Su AW, Chen Y, Wailes DH, Wong VW, Cai S, Chen AC, Bugbee WD, Sah RL. Impact insertion of osteochondral grafts: Interference fit and central graft reduction affect biomechanics and cartilage damage. J Orthop Res. 2017 Epub ahead of print.

Szczodry M, Coyle CH, Kramer SJ, Smolinski P, Chu CR. Progressive chondrocyte death after impact injury indicates a need for chondroprotective therapy. Am J Sports Med. 2009; 37:2318–2322. [PubMed: 19864505]

Torzilli PA, Deng XH, Ramcharan M. Effect of compressive strain on cell viability in statically loaded articular cartilage. Biomech Model Mechanobiol. 2006; 5:123–132. [PubMed: 16506016]

Torzilli PA, Grigiene R, Borrelli J Jr, Helfet DL. Effect of impact load on articular cartilage: cell metabolism and viability, and matrix water content. J Biomech Eng. 1999; 121:433–441. [PubMed: 10529909]

Whiteside RA, Jakob RP, Wyss UP, Mainil-Varlet P. Impact loading of articular cartilage during transplantation of osteochondral autograft. J Bone Joint Surg Br. 2005; 87:1285–1291. [PubMed: 16129760]

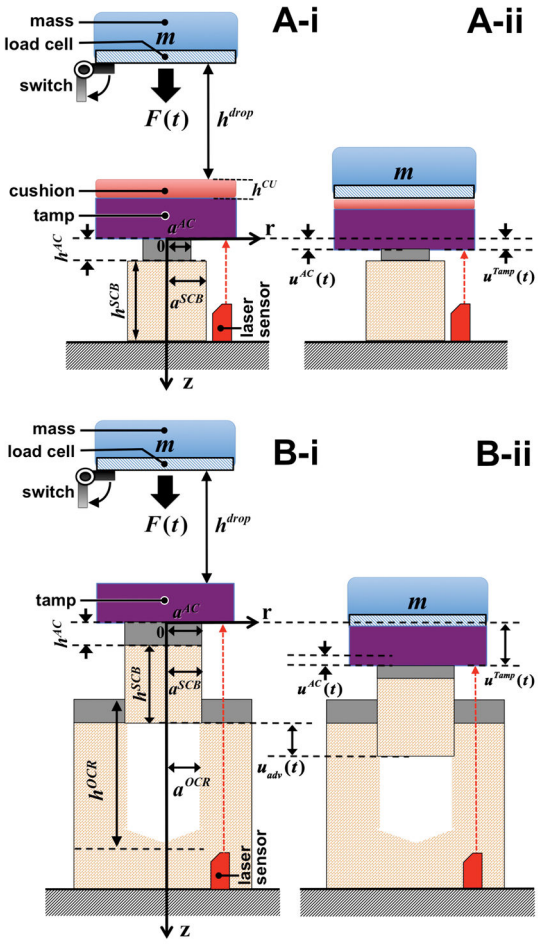

Figure 1. Schematics of impact load application and sensor measurements using drop tower apparatus

(A) Impact of isolated OsteoChondral Sample, with interposed cushion. **(B)** Insertion of OsteoChondral Graft into OsteoChondral Recipient site. (i) Mass in raised position. (ii) Mass at time (*t*) after impact. Optional cushion included in-line between the drop mass and the rigid tamp.

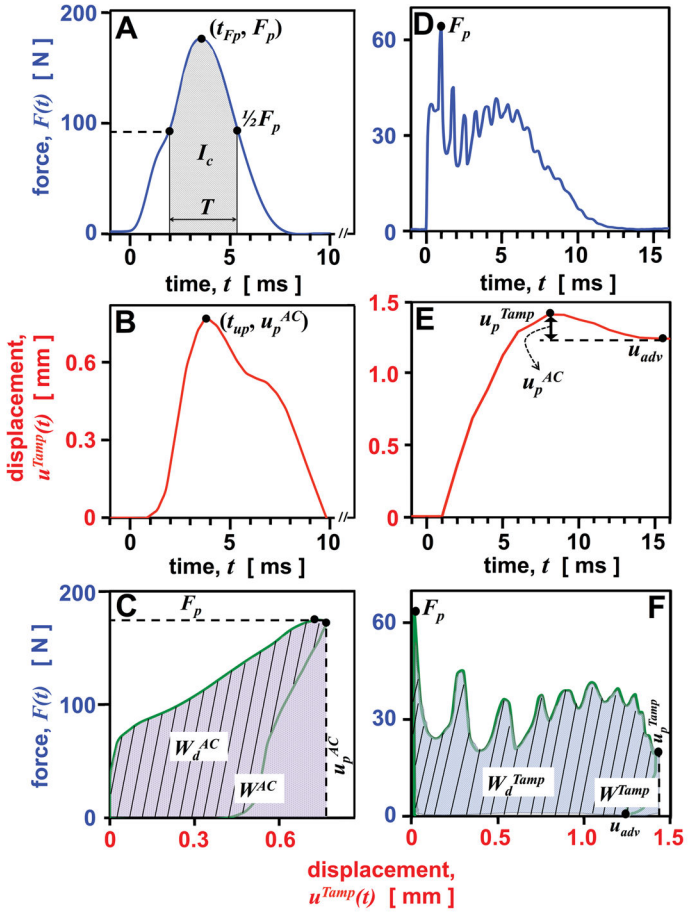

Figure 2. Mechanical variables and parameters. (A–C) Impact of isolated OCG. (D–F) Insertion of OCG into OCR

Time-dependences of **(A,D)** force and **(B,E)** displacement. **(C,F)** Energy calculations based on force as a function of displacement.

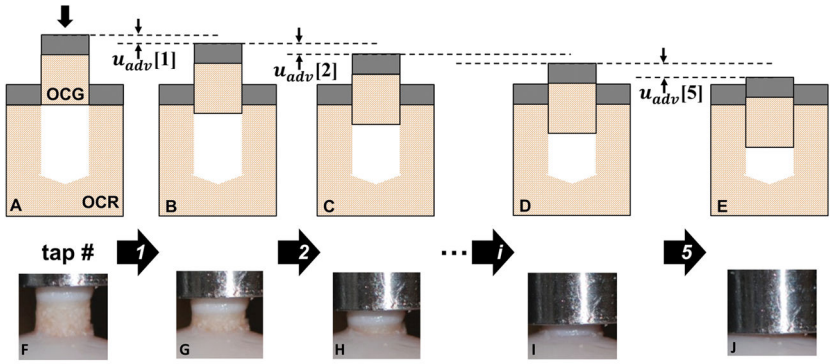

Figure 3. Schematic and images of impact insertion of OCGs and mechanical variables and parameters

Advancement of OCG into OCR, **(A, F)** starting with initial position, **(B–D, G–I)** advancing with successive taps (*i*) to **(E, J)** final (slightly proud) position after the 5th tap. Incremental OCG advancement with tap *i* is $u_{adv}[i]$.

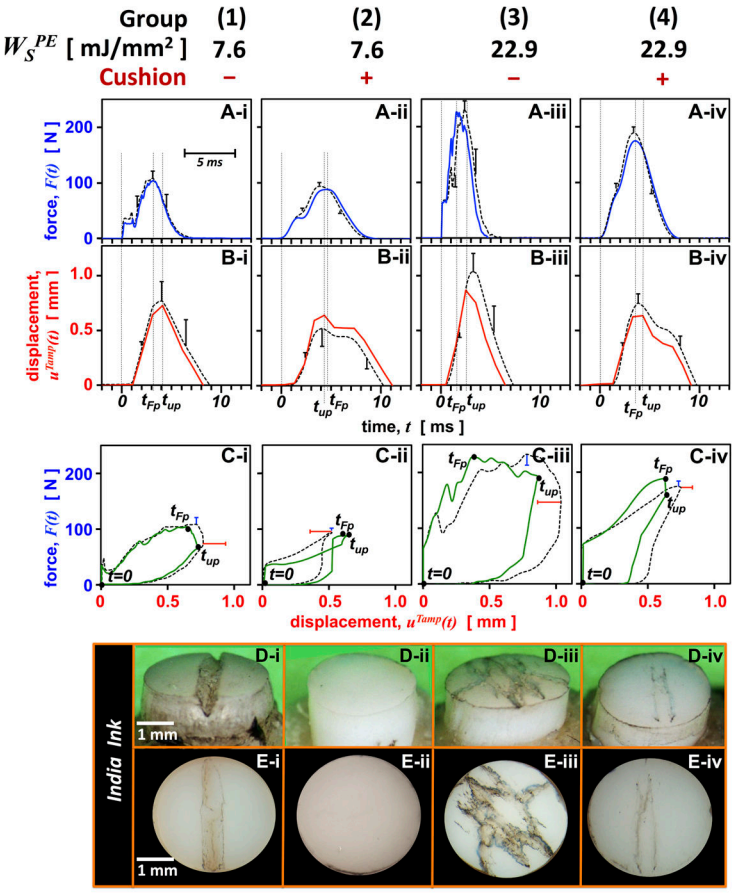

Figure 4. Effect of applied energy density (W_S^{PE}) and cushioning on impact mechanics and biological outcomes

(A) force, **(B)** displacement, **(C)** energy loop. **(D)** Oblique and **(E)** *en Face* views of articular cartilage of samples after staining with India Ink to visualize surface cracks. Experimental groups are **(i–iv)**. In **(A–C)**, solid colored lines represent a typical sample in the group, and black dashed lines represent the group mean±SD (n=6 each).

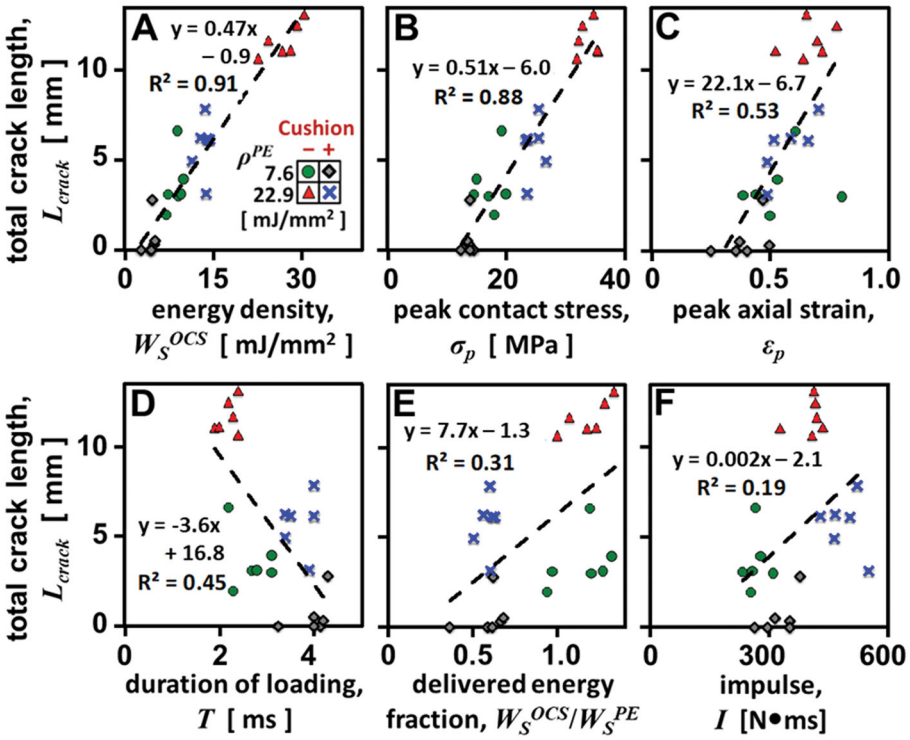

Figure 5. Regression analysis of articular cartilage damage against mechanical variables after single impact of OCG at different energy levels and with or without an interposed cushion

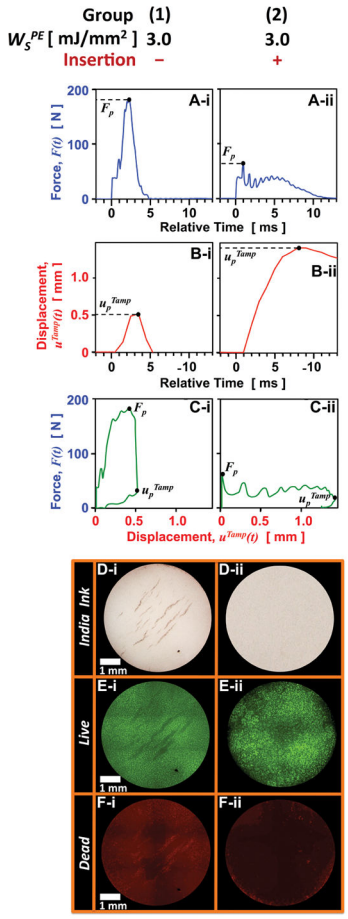

Figure 6. Effect of OCG insertion on impact mechanics and cartilage damage

Representative **(A)** force, **(B)** displacement, and **(C)** energy loop. **(D)** *En face* view of India Ink stained samples to visualize cartilage surface cracks. Chondrocyte viability was determined under fluorescence microscopy to visualize **(E)** live cells in green, and **(F)** dead cells in red. Experimental groups are **(i)** non-insertion OCG and **(ii)** OCG inserted into OCR.

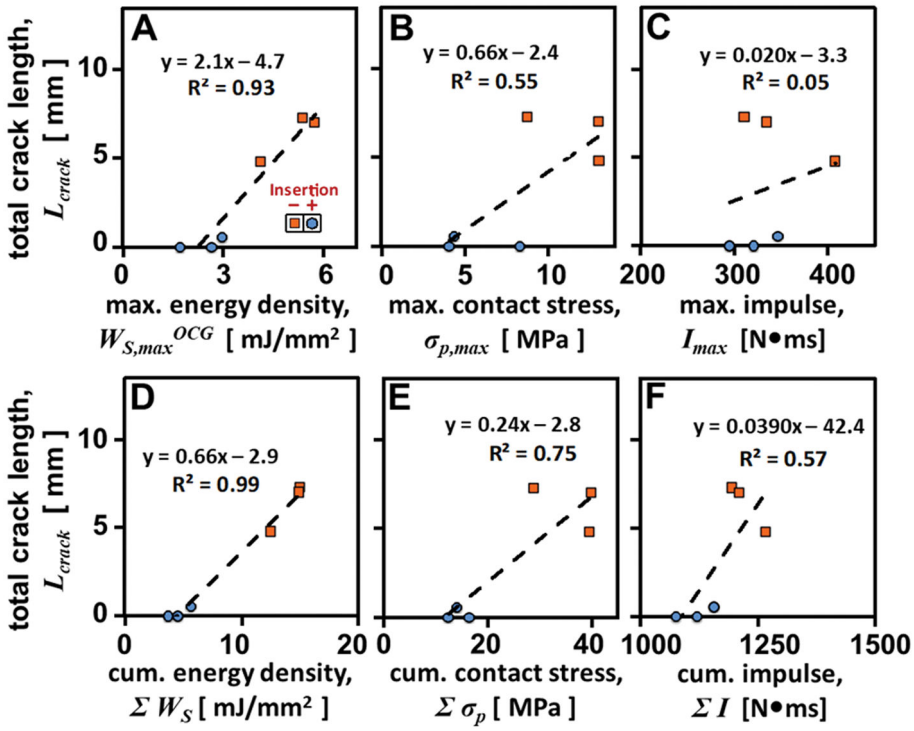

Figure 7. Regression analysis of articular cartilage damage against mechanical variables from serial impact of OCG, with or without insertion into OCR

(A–C) Maximal and **(D–F)** cumulative values.

Table 1
Biomechanical parameters and variables

Parameters and variables represent continuous numbers or integers.

parameter	definition	unit
$A^{AC}(t_{0-})$	AC surface area prior to impact	mm^2
a^{AC}	radius of AC surface of OCG	mm
a_{OCR}	radius of OCR	mm
a_{SCB}	radius of SCB of OCG	mm
$h^{AC}(t_{0-})$	thickness of AC of OCG prior to impact	mm
h^{CU}	thickness of the cushion	mm
h^{drop}	drop height for the drop mass in drop tower	mm
h^{OCR}	depth of OCR relative to cartilage surface	mm
h^{SCB}	height of SCB of OCG	mm
$[i]$	sequential tap number when inserting OCG into OCR, i=1, 2, …, 5	—
m	mass of drop mass	g

variable	definition	unit
$A^{AC}(t_{24hr+})$	AC surface area 24 hours post impact	mm^2
ε_p	peak axial strain of AC of OCG	mm/mm
$F(t)$	force applied to tamp	N
F_p	peak contact force applied on the tamp during sample impact	N
F_s	static load on OCS after impact	N
$h^{AC}(t_{24hr+})$	thickness of AC of OCG 24 hours post impact	mm
I	impulse of sample impact	N•ms
I_{max}	maximal impulse for impacts of OCG	N•ms
ΣI	cumulative impact impulse, $\sum_{i=1}^{5} I[i]$	N•ms
L_{crack}	total crack lengths on articular cartilage surface	mm
σ_p	peak contact stress during impact	MPa
$\sigma_{p,max}$	maximum of peak contact stress during sequential impacts of OCG	MPa
$\Sigma\sigma_p$	cumulative peak contact stress, $\sum_{i=1}^{5} \sigma_p[i]$	MPa
t	time relative to impact event	ms
T	duration of sample impact	ms
t_{Fp}	time at when F_p occurs	ms
t_{up}	time at when u_p occurs	ms
$u^{AC}(t)$	axial displacement of AC of OCG	mm
u_{adv}	OCG advancement distance	mm

variable	definition	unit
u_p^{AC}	peak axial compressive displacement of AC of OCG	mm
u_p^{Tamp}	peak axial displacement of the tamp	mm
$u^{Tamp}(t)$	axial displacement of the tamp	mm
V^{AC}	surface chondrocyte viability of AC of OCG post impact	%
W^{AC}	energy delivered to OCG	mJ
W^{Tamp}	energy provided by tamp to the sample	mJ
W_d	energy dissipated	mJ
W_d^{AC}	energy dissipated by AC	mJ
W_S	energy density delivered to OCG	mJ/mm^2
ΣW_s	cumulative energy density delivered to OCG samples, $\sum_{i=1}^{5} W_s[i]$	mJ/mm^2
W_S^{AC}	energy density delivered to AC	mJ/mm^2
$W_{S,d}$	energy density dissipated	mJ/mm^2
$W_{S,d}^{AC}$	energy density dissipated by AC	mJ/mm^2
$W_{S,max}$	maximum energy density delivered during sequential impacts of OCG	mJ/mm^2
W_S^{PE}	applied (potential) energy density	mJ/mm^2
$W_S^{PE,total}$	total applied energy density	mJ/mm^2

Table 2

The effect of W_S^{PE} and cushioning on mechanical and biological variables

Statistical results are indicated as *** p<0.001, ** p<0.01, * p<0.05, non-significant results presented with p value, n/a: not applicable.

W_S^{PE}[mJ/mm^2]	Cushion	h^{AC} (t_{0-}) [mm]	h^{AC} (t_{24hr+}) [mm]	A^{AC} (t_{24hr+}) [mm^2]	F_p [N]	σ_p [MPa]	t_{Fp} [ms]	T [ms]	I [N•ms]	t_{up} [ms]	u_p^{AC} [mm]	e_p^{AC}	W^{AC} [mJ]	W_d^{AC} [mJ]	W_S^{AC}[mJ/mm^2]	$W_{S,d}^{AC}$[mJ/mm^2]	$W_S^{AC}/W_S^{PE,Tot}$	L_{crack} [mm]
7.6	−	1.59±0.18	1.65±0.19	7.88±0.64	123±15	17.4±2.2	3.1±0.6	2.7±0.4	267±26	3.9±0.6	0.86±0.20	0.55±0.15	62±8	49±7	8.7±1.2	7.0±0.9	1.05±0.14	3.6±1.6
7.6	+	1.58±0.26	1.62±0.10	7.18±0.36	97±5	13.8±0.7	4.1±0.5	4.0±0.4	328±42	3.7±0.7	0.61±0.08	0.39±0.09	32±6	20±2	4.5±0.9	2.9±0.3	0.55±0.10	0.6±1.1
22.9	−	1.63±0.31	1.69±0.35	10.92±1.51	240±12	33.9±1.6	2.2±0.4	2.2±0.2	405±38	3.1±0.5	1.08±0.20	0.67±0.09	190±21	169±20	26.9±2.9	23.9±2.9	1.14±0.12	11.4±0.7
22.9	+	1.37±0.22	1.44±0.19	8.28±0.74	175±10	24.8±1.4	3.5±0.1	3.7±0.3	490±44	4.0±0.3	0.78±0.10	0.58±0.09	95±7	67±7	13.4±1.1	9.4±1.0	0.57±0.04	5.7±1.6
Effect of W_S^{PE} (p-value)		0.33	0.31	***	***	***	***	**	***	0.33	**	**	***	***	***	***	0.24	***
Effect of cushioning (p-value)		0.18	0.14	***	***	***	**	***	***	0.13	***	*	***	***	***	***	***	***
Interactive effect (p-value)		0.23	0.31	*	0.20	0.20	0.13	0.16	0.94	*	0.84	0.58	0.70	0.57	0.70	0.57	0.60	0.06
L_{crack} correlation, (R^2)		n/a	n/a	n/a	0.88 ***	0.88 ***	n/a	0.45 ***	0.19 *	n/a	0.54 ***	0.53 ***	0.91 ***	0.89 ***	0.91 ***	0.89 ***	0.38 **	n/a

Table 3

The effect of insertion and successive impacts on mechanical and biological variables

Ins: insertion, (−): impact load on isolated OCG without insertion, (+): OCG insertion into OCR. Statistical results are indicated as *** p<0.001, ** p<0.01, * p<0.05, non-significant results with p value, and n/a, not applicable. (A) Comparison for each tap, *i*. (B) Cumulative effect of 5 impacts.

Table 3A.

Study Group	Ins	tap #,	W_S^{PE}[mJ/mm^2]	F_p [N]	σ_p [MPa]	I [N•ms]	T [ms]	u_p^{Tamp} [mm]	u_{adv} [mm]	u_p^{AC} [mm]	e_p	W^{Tamp} [mJ]	W^{AC} [mJ]	W_d [mJ]	W_S^{AC}[mJ/mm^2]	$W_{S,d}$ [mJ/mm^2]	$W_S^{AC}/W_S^{PE,Tot}$
1	−	1	0.9	69±5	3.8±0.3	188±14	3.0±0.4	0.51±0.15	n/a	0.51±0.15	0.29±0.05	22±3	22±3	17±3	1.2±0.2	1.0±0.1	1.14±0.14
2	+	1	0.9	22±5	1.2±0.2	166±2	10.0±2.2	0.83±0.01	0.49±0.10	0.34±0.11	0.21±0.07	14±2	6±2	12±2	0.3±0.1	0.7±0.1	0.28±0.10
Effect of Ins (p-value)				***	***	*	**	*	n/a	0.18	0.18	*	**	0.07	**	0.07	***
1	−	2	1.3	86±11	4.7±0.6	203±19	2.6±0.4	0.53±0.13	n/a	0.53±0.13	0.30±0.04	29±4	29±4	22±5	1.6±0.2	1.2±0.3	1.08±0.14
2	+	2	1.3	36±5	2.0±0.3	202±6	8.5±1.3	0.90±0.16	0.60±0.11	0.31±0.11	0.18±0.07	21±0.4	7±2	19±1	0.4±0.1	1.0±0.0	0.23±0.075
Effect of Ins (p-value)				***	**	0.94	***	*	n/a	0.08	0.08	*	***	0.40	***	0.40	***
1	−	3	2.0	126±24	7.0±1.3	215±6	2.0±0.6	0.57±0.16	n/a	0.57±0.16	0.32±0.05	48±1	48±1	41±1	2.6±0.0	2.3±0.0	1.21±0.01
2	+	3	2.0	43±3	2.4±0.2	201±17	7.6±0.8	1.06±0.15	0.73±0.17	0.33±0.03	0.20±0.02	26±3	8±1	24±3	0.5±0.1	1.3±0.2	0.19±0.04
Effect of Ins (p-value)				**	**	0.25	**	*	n/a	*	*	***	***	**	***	**	***
1	−	4	3.0	163±36	9.0±2.0	267±8	1.9±0.5	0.59±0.21	n/a	0.59±0.21	0.33±0.08	65±7	65±7	61±5	3.6±0.4	3.4±0.3	1.13±0.11
2	+	4	3.0	58±5	3.2±0.3	229±28	6.2±1.2	1.45±0.35	0.78±0.27	0.67±0.24	0.41±0.17	42±3	20±7	40±3	1.1±0.4	2.2±0.2	0.31±0.11
Effect of Ins (p-value)				**	**	0.09	**	*	n/a	0.69	0.69	**	**	**	**	**	***
1	−	5	4.5	209±45	11.6±2.5	351±51	1.7±0.3	0.64±0.21	n /a	0.64±0.21	0.36±0.09	92±15	92±15	87±13	5.1±0.9	4.8±0.7	1.08±0.17
2	+	5	4.5	101±43	5.6±2.4	321±26	4.7±2.2	1.05±0.34	0.36±0.11	0.69±0.27	0.43±0.21	68±12	44±12	62±11	2.5±0.6	3.4±0.6	0.51±0.13
Effect of Ins (p-value)				*	*	0.43	0.06	0.15	n/a	0.83	0.83	0.08		0.06	*	0.06	*

Table 3B

Study Group	Ins	h^{AC} (t_{0-}) [mm]	$\sigma_{p,max}$ [MPa]	$\Sigma\sigma_p$ [MPa]	I_{max} [N•ms]	ΣI[N•ms]	$W_{S,max}$ [mJ/mm^2]	ΣW_S [mJ/mm^2]	L_{crack} [mm]	V^{AC} [%]
CTRL	n/a									97±3
1	−	1.76±0.24	11.6±2.5	36.1±6.3	351±51	1224±38	5.1±0.9	14.2±1.4	6.4±1.4	88±6*
2	+	1.67±0.15	5.6±2.4	14.4±2.0	321±26	1119±41	2.5±0.7	4.7±1.0	0.2±0.3	95±3
Effect of Ins (p-value)		0.61	*	*	0.43	*	*	**	***	*
L_{crack} **correlation,** (R^2)		n/a	0.55 (p=0.09)	0.75*	0.05 (p=0.67)	0.57 (p=0.08)	0.93**	0.99***	n/a	0.49 (p=0.12)